Society of Cable Telecommunications Engineers

SCTE Conference on Emerging Technologies® 2009

DOCSIS® 3.0 Upstream Channel Bonding: Performance Analysis in the Presence of HFC Noise

Ayham Al-Banna
Sr. Systems Architect, ARRIS
2400 Ogden Ave Suite 180
Lisle, IL 60532
+1 630 281 3009
Ayham.Al-Banna@arrisi.com
http://www.arrisi.com

Jim Allen
Sr. Software Engineer, ARRIS
2400 Ogden Ave Suite 180
Lisle, IL 60532
+1 630 281 3009
Jim.Allen@arrisi.com
http://www.arrisi.com

Tom Cloonan
Chief Strategy Officer, ARRIS
2400 Ogden Ave Suite 180
Lisle, IL 60532
+1 630 281 3050
Tom.Cloonan@arrisi.com

Table of Contents

Abstract

Recent studies have shown that bandwidth usage has been exponentially increasing every year since the inception of dial-up modems. Rising customers' expectations are motivating MSOs and Cable Modem Termination System (CMTS) vendors to pursue cutting-edge technologies to satisfy customers' needs. Therefore, the DOCSIS® 3.0 standard, which was developed recently, proposes different mechanisms to increase the bandwidth offered to cable customers. Among these mechanisms are expanding the upstream (US) spectrum, downstream (DS) channel bonding, and US channel bonding.

While wide, non-bonded channels can provide relatively high throughput (up to ~30 Mbps), deploying DOCSIS 3.0 US channel bonding introduces many new benefits. An obvious benefit of US channel bonding is the ability to offer customer throughput that exceeds 30 Mbps. However, there are many other benefits of US channel bonding, including statistical multiplexing gain, flexible and efficient US spectrum assignment, grow-as-you-go strategy, and better quality of service (QoS).

Although the US spectrum is limited and noisy, it can be used efficiently to offer higher data rates through US channel bonding. This is primarily because of the excellent performance obtained by US channel bonding in the presence of different HFC noise types. In this article, we closely analyze the performance of US channel bonding in the presence of Additive White Gaussian Noise (AWGN), Semi-AWGN noise, Ingress noise, and Impulse noise. We demonstrate that the performance of US channel bonding can be better than the performance of wide channels in the presence of AWGN. We also show that the performance of US channel bonding can be better than that of wide channels in the presence of Semi-AWGN, Ingress noise, and Impulse noise. In the conclusion of the analysis, we will show how US channel bonding can offer higher data rates than single wide channels.

Introduction

Through the creation of the DOCSIS 3.0 specifications, CableLabs® and innovative researchers within the Cable Industry have worked together to define and standardize many powerful new technologies that are now beginning to appear in many next-generation CMTS and CM products. One of the most intriguing technologies included in the DOCSIS 3.0 specifications is known as "Channel Bonding," and it promises to offer many bandwidth-oriented benefits for both Downstream High-Speed Data (HSD) transmissions and Upstream HSD transmissions.

To date, most of the focus surrounding the delivery and deployment of Channel Bonding has focused on the Downstream flavor of this capability. As a result, that particular form of DS Channel Bonding is already being deployed in the field. However, many cable operators are beginning to show more and more interest in the deployment of US Channel Bonding in the upcoming year. As a result, this paper will focus on US Channel Bonding.

In its most simplistic form, Channel Bonding attempts to provide more bandwidth capacity to each CM subscriber than is currently permitted using a single DOCSIS 2.0 DS channel and a single DOCSIS 2.0 US channel. Channel Bonding accomplishes this task by permitting traffic to

a single CM subscriber to traverse across M available DOCSIS DS channels and by permitting traffic from a single CM subscriber to traverse across N available DOCSIS US channels (M>0 and N>0). For DOCSIS 2.0 systems, M and N were both limited to a value of one (1). For DOCSIS 3.0 systems, the use of Channel Bonding can permit both M and N to be values greater than one (1). In the system of **Fig. 1**, Channel Bonding is provided using M=4 parallel DS Channels and N=4 parallel US Channels between the DOCSIS 3.0 CMTS and the DOCSIS 3.0 CM, while the legacy (pre-DOCSIS 3.0) CM is limited to using only one DS Channel and one US Channel. As a result, the DOCSIS 3.0 CM has access to 4*~40 Mbps=~160 Mbps of DS bandwidth capacity and 4*~30 Mbps=~120 Mbps of US bandwidth capacity, whereas the legacy CM only has access to ~40 Mbps of DS bandwidth capacity and ~30 Mbps of US bandwidth capacity. If all four DS Channels are used to transport data to the CM, then the set of those four DS Channels is called a DS Bonding Group. If all four US Channels are used to transport data from the CM, then the set of those four US Channels is called an US Bonding Group.

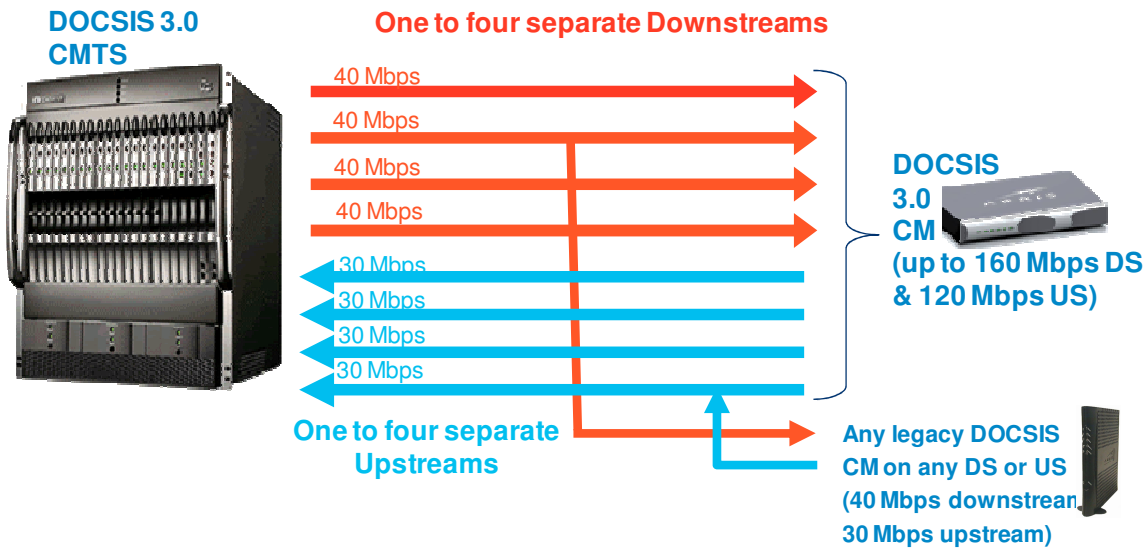

Fig. 1- Downstream and Upstream Channels for DOCSIS 3.0 Bonded CMs and Legacy Non-Bonded CMs

To understand the true benefits provided by the Channel Bonding solution shown in **Fig. 1**, it is important to understand the current capabilities of existing DOCSIS systems. In current DOCSIS 1.x and DOCSIS 2.0 systems, a single CM can connect (via the ranging and registration processes) to only M=1 DOCSIS DS channel and can connect (via the ranging and registration processes) to only N=1 DOCSIS US channel. As a result, current DOCSIS 2.0 systems hard-limit the DS bandwidth to a single CM to be at most 42.884296 Mbps in North America and Asia (Annex B and C channels with 256QAM over 6 MHz channels) and hard-limit the DS bandwidth to a single CM to be at most 55.616 Mbps in Europe (Annex A channels with 256QAM over 8 MHz channels). Current DOCSIS 2.0 systems hard-limit the US bandwidth to a single CM to be at most 30.72 Mbps in North America, Asia, and Europe (channels with 64QAM running over 6.4 MHz channels). All of these bandwidths are “raw” bandwidths in the sense that we have not deducted for the relatively small overheads that exist on the DOCSIS channels.

By using DS Channel Bonding techniques, an MSO can use M DOCSIS DS Channels to yield "raw" DS bandwidths of M*42.884296 Mbps to North American and Asian CM subscribers and M*55.616 Mbps to European CM subscribers. Similarly, by using US Channel Bonding techniques, an MSO can use N DOCSIS US channels to yield "raw" US bandwidths of M*30.72 Mbps to North American, Asian, and European CM subscribers. **Table 1** and **Table 2** illustrate the resulting "raw" bandwidths for various values of M and N.

M	Raw Downstream Bandwidth for Annex B and C	Raw Downstream Bandwidth for Annex A
1	~43 Mbps	~56 Mbps
2	~86 Mbps	~111 Mbps
3	~129 Mbps	~167 Mbps
4	~171 Mbps	~222 Mbps
5	~214 Mbps	~278 Mbps
6	~257 Mbps	~334 Mbps
7	~300 Mbps	~389 Mbps
8	~343 Mbps	~445 Mbps

Table 1- Raw Downstream Bandwidth (Mbps) vs. M assuming 256QAM

N	Raw Upstream Bandwidth
1	~31 Mbps
2	~61 Mbps
3	~92 Mbps
4	~123 Mbps
5	~154 Mbps
6	~184 Mbps
7	~215 Mbps
8	~246 Mbps

Table 2- Raw Upstream Bandwidth (Mbps) vs. N assuming 64QAM in 6.4 MHz channels

It should be noted that there must be adequate HSD spectrum available to support the M DS Channels and N US Channels to obtain the bandwidths shown in the tables above. MSOs are

likely to run into business case issues in obtaining DS spectrum for DS Channel Bonding, as many business case discussions involving spectrum allocation maps will be required before MSOs willingly donate DS Channels to their DOCSIS tiers from their video tiers. The story is somewhat different in the US direction. Given current HFC plant designs, MSOs are likely to run into hard spectral limits on their US spectrum as they try to allocate US spectrum for US Channel Bonding. These limits will likely exist for some time until MSOs look to other techniques (like the use of mid-split architectures or spectral overlay architectures with larger US passbands) to augment the US spectral widths. For example, the typical 5-42 MHz spectrum dedicated to US dataflow in most North American cable HFC plants would only permit an MSO to place (42 MHz – 5 MHz)/(6.4 MHz per US channel) = ~5 US Channels on the HFC plant if DOCSIS 2.0 6.4 MHz channels are used. As a result, MSOs will likely need to be careful when deciding how to use and deploy these five precious (and limited) US Channels in a Channel Bonding environment. Since noisy environments are likely to be found in the US regions of the spectrum where these five channels may exist, MSOs must deal with that added layer of complexity when calculating the available user bandwidth capacity within an US Bonding Group.

That fact brings us to the topic of this paper. All of the Channel Bonding throughput calculations performed above assume that the channels can be logically aggregated together without considering the effects of noise on the channel. In essence, all of the throughput calculations above assumed that the channels being bonded together were essentially noise-free, and that noise mitigation techniques would not consume any of the channel bandwidth. The authors of this paper became interested in exploring the throughputs associated with bonded channels when noise of varying types was present and accounted for on the US Bonded Channels. In particular, the authors studied the effects of several different types of noise on the individual and overall performance of US Bonded Channels. These noise types included all of the different types of noise that are likely to be found within the US spectrum, including Additive-White-Gaussian Noise (AWGN), Semi-Additive White Gaussian Noise, narrowband Ingress Noise, and Impulse (or burst) Noise.

Calculation of Packet Error Rates (PER) for US Channels with these different noise types present was the first step in the analysis. But knowledge of the PER on an US Channel is not sufficient for determining the impact on the subscriber's US throughput (bonded or non-bonded). Instead, the authors chose to specify an acceptable PER for each channel, and then they automatically sampled a very large array of settings for the various DOCSIS noise mitigation techniques to identify an optimal noise mitigation setting for the particular noise on the channel that would achieve the desired PER. The resulting noise mitigation techniques used by that optimal setting would inevitably limit the total available throughput associated with the noise on that channel. As a result, the actual US Channel throughputs and the actual US Bonding Group throughputs could be calculated and compared for the different types of noise. This Bonding Group bandwidth is typically reduced from the "raw" throughput numbers calculated above. The results of these studies are presented below.

PER Calculations for Different Noise Types within the Upstream Spectrum

There are several different types of noise that are likely to exist within the US spectrum. These include Additive White Gaussian Noise (AWGN), Semi-Additive White Gaussian Noise, narrowband Ingress Noise, and Impulse (or burst) Noise. Being able to determine the PER for a particular channel with a particular type of noise was an important part of this study. The manner in which these PERs were calculated for each of the noise types is outlined below.

Additive White Gaussian Noise and Semi-Additive White Gaussian Noise

Additive White Gaussian Noise exists in all cable plants. It results from many natural sources, including the thermal vibrations of atoms in the cable as well as the radiation generated from warm objects or celestial sources which can couple into the cable at connectors. It is assumed to be a wideband noise, with a constant power spectral density across the entire spectrum. The amplitude of the random noise has a probability density function that tends to be Gaussian in shape, and it occurs continuously across time. As a result, if its amplitude is large enough at times, it can randomly affect (and corrupt) any symbol being transmitted across the US Channel. Typically, it does so with a low probability of error. Calculating this probability of error is important if we are going to change the US channel settings to yield a particular probability of error level. An example of Additive White Gaussian Noise is shown in both the time domain and the frequency domain in **Fig. 2**.

Fig. 2- Example of AWGN in the Time Domain and Frequency Domain

In an US QAM channel, each QAM symbol is used to encode multiple bits of the US bit-stream. Each M-ary QAM symbol encodes m=log2(M) bits, so 16QAM implies that each symbol transmitted across the communication channel will carry four bits. Depending on the four-bit pattern that is being transmitted, the waveform a(t) will have a different shape. The probability of a particular symbol being interpreted incorrectly (the Probability of a symbol error or Perr) at the output is a function of two fundamental values: the average energy per symbol Eavg within each of the symbols and the noise power spectral density of the random noise signal n(t).

In particular, one can determine the probability of error for each of the signal modulation types permitted in a TDMA/ATDMA system by first determining the average energy per symbol (Eavg) and the noise power spectral density level. (Note: It can also be shown that similar results are found for SCDMA systems). The noise power spectral density level is equated to a level of $\frac{N_o}{2}$ W/Hz (assuming that the noise has Additive White Gaussian Noise characteristics, which has a constant power spectral density level ($\frac{N_o}{2}$) at all frequencies in both the positive and negative frequency spectra).

For example, assume that the average power of the transmitted TDMA/ATDMA signal is Pavg. Thus, Pavg is a value that is specified in the CMTS MIB.

This variable is in units of power (Watts, microwatts, dBm, etc.). Conversion between these different units can occur quite easily using the following formulae:

dBm = 10*log10(Pavg), where Pavg is in mW

$P_{avg} = 10^{\frac{dBm}{10}}$, where Pavg is in mW

dBmV = dBm + 48.8

dBm = dBmV – 48.8

The average energy per symbol (Eavg) is therefore given by

$$E_{avg} = P_{avg} \cdot T_a , \quad (1)$$

where Ta is the symbol period.

The average energy per bit (Eb) is therefore given by:

$$E_b = \frac{E_{avg}}{\#\ of\ bits\ /\ symbol} = \frac{P_{avg} \cdot T_a}{\#\ of\ bits\ /\ symbol} . \quad (2)$$

Some very interesting relationships between energy per symbol (Eavg), noise power spectral density level (½)N0, signal power (Pavg), and noise power (N) can be defined for different modulation types and different channel widths (symbol rates). The symbol duration (Ta) and the symbol rate (Rsymb) are related by the simple equation:

$$T_a = \frac{1}{R_{symb}} . \quad (2a)$$

So we can re-write Eq. (1) as:

$$E_{avg} = \frac{P_{avg}}{R_{symb}} . \quad (2b)$$

Thus, Pavg can be written as:

$$P_{avg} = E_{avg} \cdot R_{symb} . \quad (2c)$$

For a channel with a channel width (in the positive frequency spectrum) of W, the channel will also consume a region of width W in the negative frequency spectrum, so the total portion of the spectrum (positive and negative) consumed by the channel is 2W. Thus, the total noise power (N) within the region of the spectrum occupied by the channel is given by:

$$N = \frac{N_o}{2} \cdot 2W = N_o \cdot W . \quad (2d)$$

This leads to the equation:

$$N_o = \frac{N}{W}, \qquad \text{(2dd)}$$

which is a constant value for AWGN.

Thus, the signal-to-noise ratio (SNR) within the pass-band of interest is given by:

$$SNR = \frac{Pavg}{N} = \frac{E_{avg} \cdot R_{symb}}{N_o \cdot W}. \qquad \text{(2e)}$$

For all of the US channel widths defined in DOCSIS, the symbol shaping employs a Square Root Raised Cosine filter with alpha=0.25, so the ratios of the resulting channel widths (W) to the symbol rate (Rsymb) is a constant value of 1.25. As an example, if W=3.2 MHz and Rsymb=2.56 Msymbol/sec, then W/Rsymb=1.25. Similarly, if W=200 kHz and Rsymb=160 ksymbol/sec, then W/Rsymb=1.25. Substituting this constant value into Eq. (2e) yields:

$$SNR = \frac{E_{avg}}{1.25 \cdot N_o} \qquad \text{(2f)}$$

or

$$\frac{E_{avg}}{N_o} = 1.25 \cdot SNR. \qquad \text{(2ff)}$$

The SNR value described in Eq. (2ff) is taken after the band-pass filter on the channel receiver, so a widening of the channel width will typically lead to an increase in the noise power N. If the signal power (Pavg) is maintained at the same level on a channel (which is commonly done by craft personnel when channel widths are altered), then the resulting SNR will be reduced and the symbol (and packet) error rate will be increased as the channel width (and symbol rate) is increased. This effect is illustrated in **Fig. 3a** for several 16QAM channels with different channel widths in the presence of the same AWGN .

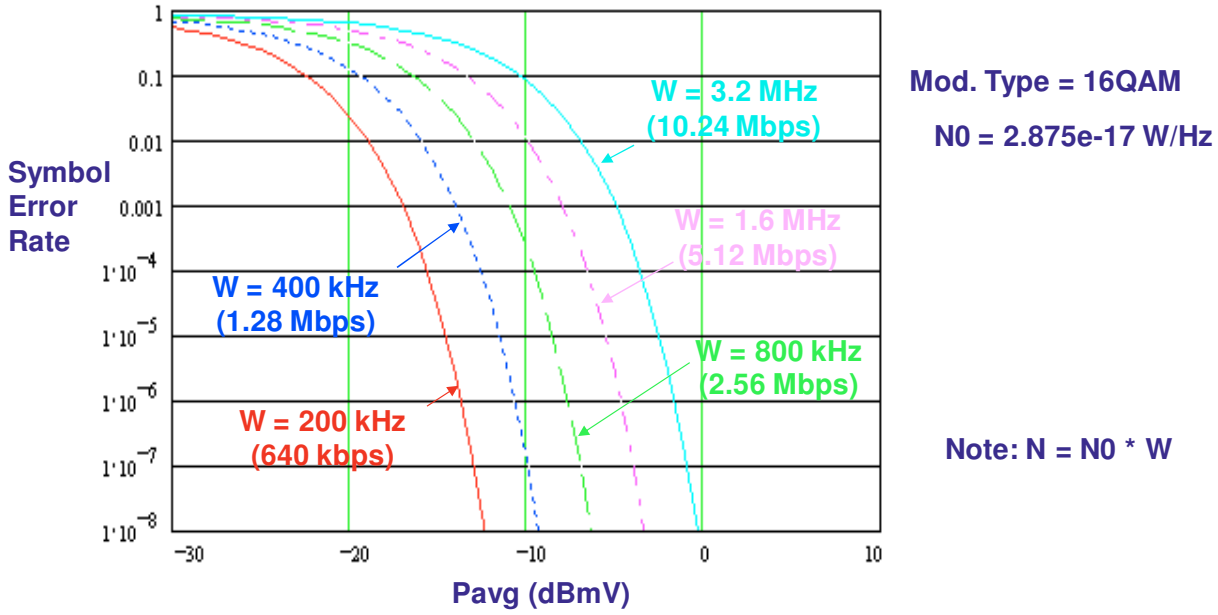

Fig. 3a- Symbol Error Rates for 16QAM Channels with Different Channel Widths in the presence of AWGN

One can also calculate the value of $\frac{E_{avg}}{N_o}$, which is important in many of the formulae below.

(Note: We use Eavg instead of Eb, which is normally used in text books, because it is the energy in the symbol Eavg that is used to determine symbol error rate- not the energy per bit given by Eb). In particular,

$$\frac{E_{avg}}{N_o} = \frac{P_{avg} / R_{symb}}{N_o} = \frac{P_{avg}}{N_o \cdot R_{symb}}. \qquad (2g)$$

Pavg can be measured directly at the CMTS (or can be inferred from configured settings), and N0 can be calculated for most cable plants as shown at the end of this section.

For M=4 QPSK (which has log2(M)=log2(4)=2 bits per symbol and Eavg=2*Eb), it can be shown that the M=4 QPSK system will experience a probability of symbol error (Perr4) given by [Pro]:

$$P_{err4} = 2 \cdot Q\left[\sqrt{\frac{E_{avg}}{N_o}}\right] \cdot \left(1 - \frac{1}{2} \cdot Q\left[\sqrt{\frac{E_{avg}}{N_o}}\right]\right), \qquad (3a)$$

where [Pro],

$$Q[x] = \frac{1}{2} \cdot erfc\left(\frac{x}{\sqrt{2}}\right) \qquad (3b)$$

and erfc(x) is defined as the well-known complementary error function, which is tabulated in Tables G.1 and G.2 on pg. 540 of [Str].

For M-ary QAM (which has log2(M) bits per symbol and Eavg=log2(M)*Eb), it can be shown that the M-ary QAM system will experience a probability of symbol error (PerrM, M=16) given by (pg. 278 in [Pro]):

$$P_{errM} = 1 - \left(1 - 2 \cdot \left(1 - \frac{1}{\sqrt{M}} \right) \cdot Q\left[\sqrt{\frac{3 \cdot E_{avg}}{(M-1) \cdot N_o}} \right] \right)^2 \qquad (4a)$$

where [Pro],

$$Q[x] = \frac{1}{2} \cdot erfc\left(\frac{x}{\sqrt{2}} \right) \qquad (4b)$$

and erfc(x) is defined as the complementary error function, which is tabulated in Tables G.1 and G.2 of [Str].

A simple substitution of Eq. (2f) into Eq. (4a) yields the resulting equation:

$$P_{errM} = 1 - \left(1 - 2 \cdot \left(1 - \frac{1}{\sqrt{M}} \right) \cdot Q\left[\sqrt{\frac{3.75 \cdot SNR}{(M-1)}} \right] \right)^2 \qquad (4c)$$

It should be noted that Eq. (4c) is strictly correct only when M is a perfect square (ex: 4, 16, 64, 256, 1024). However, it can be shown that Eq. (4c) can also be used as an approximation to the symbol error rate for other values of M (ex: 8, 32, 128, 512). However, we choose to use a simpler approximation to PerrM for these other values of M. In particular, when M is not a perfect square, we will assume that PerrM can be upper bounded by:

$$P_{errM} = 1 - \left(1 - 2 \cdot Q\left[\sqrt{\frac{3.75 \cdot SNR}{(M-1)}} \right] \right)^2 \qquad (4d)$$

as recommended in [Pro].

The different modulation types (QPSK, 8QAM, 16QAM, 32QAM, 64QAM) used in DOCSIS each experience a different symbol error rate (PerrM) in the presence of a particular SNR. In a particular SNR environment, lower-order modulation types (ex: QPSK or 8QAM) will experience lower error rates than higher-order modulation orders (ex: 16QAM, 32QAM, or 64QAM), as illustrated in **Fig. 3b**.

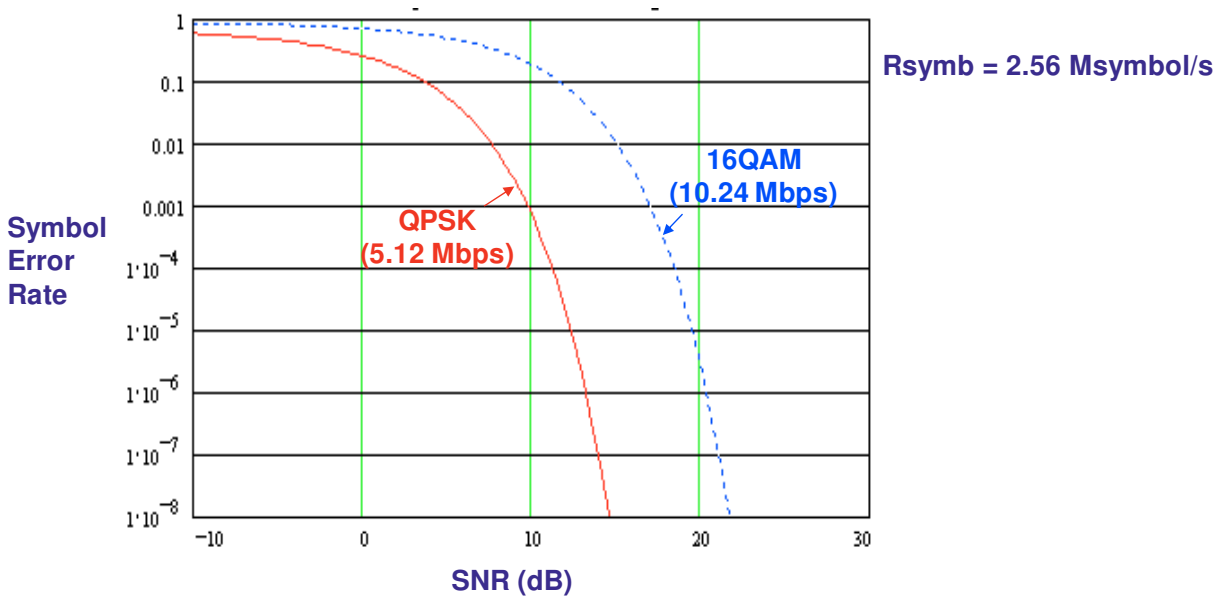

Fig. 3b- Symbol Error Rates vs. SNR for QPSK and 16QAM Channels with 3.2 MHz Channel Width in the presence of AWGN

Once the symbol error rate PerrM (M>4) has been calculated, we can easily find transformations to yield the equivalent error rates for differently-sized "chunks" of data. In particular, it may be beneficial to be able to specify the equivalent bit error rates, the equivalent byte error rates, the equivalent PER, and the equivalent FEC codeword error rate.

Let us begin by specifying a few new terms. Let Pbit_errM be the probability of a bit error occurring, and let Pbit_okM be the probability that a bit is transmitted without error. Let Pbyte_errM be the probability of a byte error occurring, and let Pbyte_okM be the probability that a byte is transmitted without error. Let Ppkt_errM be the probability of a packet error occurring, and let Ppkt_okM be the probability that a packet is transmitted without error. Let Pcodeword_errM be the probability of a Reed-Solomon FEC codeword error occurring, and let Pcodeword_okM be the probability that a Reed-Solomon FEC codeword is transmitted without error.

Let us identify the probability that a symbol for QPSK (M=4) or M-ary QAM is transmitted without error as PokM. Thus, the probability that a symbol is transmitted without error can be defined to be:

$$PokM=(1- PerrM) \quad (4e)$$

In addition, it can be shown that:

$$Pbit\_okM=(1- Pbit\_errM) \quad (4f)$$
$$Pbyte\_okM=(1- Pbyte\_errM) \quad (4g)$$
$$Ppkt\_okM=(1- Ppkt\_errM) \quad (4h)$$
$$Pcodeword\_okM=(1- Pcodeword\_errM) \quad (4i)$$

The equivalent bit error rate Pbit_errM can be determined from the symbol error rate PerrM by recognizing the fact that a symbol contains log2(M) bits, and a symbol will be transmitted without error only if all of the log2(M) bits were transmitted without error. Thus, it can be shown that:

$$P_{okM} = \left(P_{bit\_okM}\right)^{\log_2(M)} \quad (4j)$$

$$P_{okM} = \left(1 - P_{bit\_errM}\right)^{\log_2(M)}. \quad (4k)$$

If Pbit_errM is small (which is usually the case), then Eq. (4k) can be approximated (using a power series expansion)* by:

PokM ~ 1 - log2(M)*Pbit_errM. (4l)

Algebraic manipulation of Eq. (4l) results in the desired result for the bit error rate (Pbit_errM) in terms of the symbol error rate (PerrM):

Pbit_errM = (1 – PokM)/log2(M) (4m)
Pbit_errM = (PerrM)/log2(M). (4n)

Once the bit error rate (Pbit_errM) has been calculated, it is easy to create an expression for the byte error rate (Pbyte_errM). The equivalent byte error rate Pbyte_errM can be determined from the bit error rate Pbit_errM by recognizing the fact that a byte contains 8 bits, and a byte will be transmitted without error only if all of the 8 bits within the byte were transmitted without error. Thus, it can be shown that:

$$P_{byte\_okM} = \left(P_{bit\_okM}\right)^{8} \quad (4o)$$

$$P_{byte\_okM} = \left(1 - P_{bit\_errM}\right)^{8} \quad . \quad (4p)$$

If Pbit_errM is small (which is usually the case), then Eq. (4p) can be approximated (using a power series expansion) by:

Pbyte_okM ~ 1 – 8*Pbit_errM. (4pp)

Algebraic manipulation of Eq. (4pp) results in the desired result for the byte error rate (Pbyte_errM) in terms of the symbol error rate (PerrM):

Pbyte_okM = 1 – 8*{PerrM/log2(M)}. (4q)
1 – Pbyte_errM = 1 - 8*{PerrM/log2(M)}. (4r)
Pbyte_errM = 8*{PerrM/log2(M)}. (4s)

Once the byte error rate (Pbyte_errM) has been calculated, it is also easy to create an expression for the PER (Ppkt_errM). The equivalent PER Ppkt_errM can be determined from the byte error rate Pbyte_errM by recognizing the fact that a packet contains Z bytes, and a packet will be transmitted without error only if all of the Z bytes within the packet were transmitted without error. Thus, it can be shown that:

$$P_{pkt\_okM} = \left(P_{byte\_okM}\right)^{z} \quad (4t)$$

$$P_{pkt\_okM} = \left(1 - P_{byte\_errM}\right)^{z}. \quad (4u)$$

If Pbyte_errM is small (which is usually the case), then Eq. (4u) can be approximated (using a power series expansion) by:

Ppkt_okM ~ 1 – Z*Pbyte_errM. (4v)

Algebraic manipulation of Eq. (4v) results in the desired result for the PER (Ppkt_errM) in terms of the symbol error rate (PerrM):

Ppkt_okM = 1 – Z*{8*PerrM/log2(M)}. (4w)
1 – Ppkt_errM = 1 – Z*{8*PerrM/log2(M)}. (4x)
Ppkt_errM = Z*{8*PerrM/log2(M)}. (4y)

Furthermore, it can be shown that:

Ppkt_errM = Z*{8*Pbit_errM}. (4z)

The value of N0 in the equations above is defined to be 2*(the variance of the random noise signal n(t)). The noise signal n(t) was added to the communication channel between the transmitter and the receiver, and it is usually assumed that this noise signal is an Additive White Gaussian noise (AWGN) process. According [Pro], the power spectral density (PSDawgn(f)) of an AWGN process is given by the constant value of 0.5*N0 Watts/Hz for all frequencies. The actual power spectral density (PSDact(f)) on a cable plant will likely be similar to the power spectral density of an ideal AWGN process, but it may not exactly match the AWGN power spectral density. Thus, the actual power spectral density of the noise can be approximated by sampling the channel in the absence of a source signal for a period of time T. (Note: This can be accomplished in a CMTS by scheduling burst intervals with null SIDs). This sampling yields a truncated version of the noise signal n(t). The next step in the process of approximating the actual power spectral density requires the calculation of the corresponding Fourier Transform N(f) for the truncated version of n(t). According to [Str], the approximation for the PSDact(f) is then given by:

$$PSD_{act}(f) = \frac{1}{T} \cdot \left|N(f)\right|^{2}, \quad (5)$$

where $|x|$ represents the magnitude of the value x.

It should be noted that PSDact(f) may not end up being a constant across all frequencies — i.e., it may not end up being a power spectral density corresponding to an AWGN process. However, most of the formulae in the literature assume that the power spectral density does indeed correspond to an AWGN process. Thus, it would be beneficial if we could determine a technique for converting the actual power spectral density into an AWGN power spectral density whose characteristics are a "best match" to the characteristics of the actual power spectral density. In this paper, we will make the simplifying assumption that the "best match" AWGN power spectral density will have the same power within the pass-band of interest as the actual power spectral density. In other words, we will use a form of Parseval's Theorem to ensure that the power within both power spectral densities are the same. If the pass-band of interest for the actual power spectral density extends from f1 (w1) to f2 (w2) in the positive frequency spectrum and from –f1 (-w1) to –f2 (-w2) in the negative frequency spectrum, then it can be shown that the power in the pass-band of interest for the AWGN power spectral density is given by:

$$P_{act} = \frac{1}{2\pi}\int_{-\omega_2}^{-\omega_1} PSD_{act}(\omega)d\omega + \frac{1}{2\pi}\int_{\omega_1}^{\omega_2} PSD_{act}(\omega)d\omega \qquad (6)$$

which can also be written as:

$$P_{act} = \int_{-f_2}^{-f_1} PSD_{act}(f)df + \int_{f_1}^{f_2} PSD_{act}(f)df \qquad (7)$$

Since frequency f (in Hz) and radian frequency w (in radians/sec) are related by w=2*pi*f. (Note: The integrals can be approximated by a summation of power spectral density samples multiplied by the sample width delta).

If the pass-band of interest for the AWGN power spectral density extends from f1 (w1) to f2 (w2) in the positive frequency spectrum and from –f1 (-w1) to –f2 (-w2) in the negative frequency spectrum, then it can be shown that the power in the pass-band of interest for an AWGN power spectral density is given by:

$$\begin{aligned} P_{awgn} &= \frac{1}{2\pi}\int_{-\omega_2}^{-\omega_1} PSD_{awgn}(\omega)d\omega + \frac{1}{2\pi}\int_{\omega_1}^{\omega_2} PSD_{awgn}(\omega)d\omega \\ &= \frac{1}{2\pi}\int_{-\omega_2}^{-\omega_1} \frac{N_o}{2}d\omega + \frac{1}{2\pi}\int_{\omega_1}^{\omega_2} \frac{N_o}{2}d\omega \qquad (8) \\ &= \frac{1}{2\pi}(\omega_2 - \omega_1)N_o \end{aligned}$$

which can also be written as:

$$\begin{aligned} P_{awgn} &= \int_{-f_2}^{-f_1} PSD_{awgn}(f)df + \int_{f_1}^{f_2} PSD_{awgn}(f)df \\ &= \int_{-f_2}^{-f_1} \frac{N_o}{2}df + \int_{f_1}^{f_2} \frac{N_o}{2}df \\ &= (f_2 - f_1)N_o \end{aligned} \tag{9}$$

Thus, within this paper, we will determine the value of N0 in a "best-match" AWGN power spectral density by ensuring that Pawgn=Pact, which results in the relationship:

$$N_o = \frac{\int_{-f_2}^{-f_1} PSD_{act}(f)df + \int_{f_1}^{f_2} PSD_{act}(f)df}{f_2 - f_1} \tag{10}$$

which is the same result as defined in Eq. (2dd).

Similar results were derived for Semi-Additive White Gaussian Noise, which has a non-flat response across the frequency spectrum as shown in **Fig. 3c**. This noise type is quite similar to AWGN, but it tends to have uniform energy distributed across only a portion of the spectrum.

Fig. 3c- Semi-Additive White Gaussian Noise in Frequency Domain

Narrowband Ingress Noise

Narrowband Ingress Noise exists on many cable plants. It results from many sources, including waveforms coupled into the cable from nearby power lines and signal distortions created by common path distortion, composite second order distortion, and composite triple beat. Ingress Noise tends to be continuous in time, and it tends to be a narrowband noise centered around a single frequency. An example of Narrowband Ingress Noise is shown in both the time domain and the frequency domain in **Fig. 4**.

Fig. 4- Example of Narrowband Ingress Noise in the Time Domain and Frequency Domain

As a result, the presence of Ingress Noise tends to distort the symbols and tends to degrade the output of the receiver's matched filter for all of the symbols transiting across a particular US Channel. The symbol distortion resulting from the presence of Ingress Noise tends to increase the probability of a symbol error, especially when it is combined with the aforementioned AWGN. The authors found that one could calculate the resulting probability of error when Ingress Noise was present by effectively increasing the value of the Noise component in the SNR equations above. While this data is interesting, most MSOs enable proprietary CMTS Ingress Cancellation techniques to suppress the occurrence of the Ingress Noise spikes in the frequency domain. While details on the Ingress Noise Cancellation techniques are proprietary, it is generally understood that one can often model the Ingress Noise Cancellation techniques using narrowband spectral filters. Thus, if Ingress Cancellation techniques on the CMTS are enabled, the authors found that one could approximate the resulting SNR on the channel by placing appropriately sized "notch filters" within the frequency spectrum of both the signal's Discrete Fourier Transform and the noise's Discrete Fourier Transform. Calculating the resulting (diminished) signal power via the power spectral density and calculating the resulting (diminished) noise power via the power spectral density yields a new SNR value for the signal and noise functions that are output from the notch filter. Using this value in the PER formulae listed above yields a good approximation to the PERs witnessed in many CMTSs. Usually, the insertion of the notch filter will yield a reduction in the PER, by effectively decreasing the Noise component more than the Signal component in the SNR calculation.

Impulse (Burst) Noise

Impulse Noise (aka Burst Noise) exists on many cable plants. It is especially common within the frequency spectrum below 20 MHz. It can result from many sources, but it is usually created by a signal coupling into the cable from the contacts on a nearby rotating motor. Impulse Noise tends to manifest itself as discrete bursts of energy in the time domain. These discrete bursts can be quite short, with burst-on periods ranging from 100 nsec to 100 msec in duration. These burst-on periods are often pseudo-periodic in nature, with periods oftentimes ranging from 1 usec to 10 msec. This type of signal tends to generate a wideband noise signal in the frequency domain. An example of Impulse Noise is shown in both the time domain and the frequency domain in **Fig. 5**.

Fig. 5- Example of Impulse Noise in the Time Domain and Frequency Domain

The presence of Impulse Noise tends to degrade the output of the receiver's matched filters for all symbols in the US Channel that occur whenever the noise burst energy is present. This tends to increase the probability of a symbol error at discrete epochs of time. This effect tends to cause an increase in the PERs for the US Channel. Approximations for the increased PER can be created by determining the number of symbols that are corrupted within a single period of an Impulse Noise Signal.

Calculating the Final Packet Error Rates in a DOCSIS Upstream Channel

In the previous sections, the discussion focused on techniques for calculating the PERs that would be experienced in a particular channel with a particular type of noise and a particular DOCSIS signal level. The PER for each type could be calculated if one could determine the SNR from signal and noise samples. In the absence of other noise mitigation techniques, the Aggregate PER that one might expect to find on a channel with the different noise types mixed together would be approximated by the sum of the PER for AWGN (or Semi-Additive White Gaussian Noise or Ingress Noise) and the PER for Impulse Noise. If Ingress Cancellation is enabled, the aforementioned affect of the notch filter must be factored into the PER for Ingress Noise.

If DOCSIS offered no other noise mitigation tools, then that would be the end of the calculation. However, DOCSIS offers many other US noise mitigation tools that can be used to help improve the resultant PER at the DOCSIS receiver in the CMTS. Many of the different DOCSIS noise mitigation tools are outlined in **Table 3** below.

	AWGN	Ingress	Impulse
- 24-tap Pre-equalization	some	some	some
- RS-FEC	X	X	X
- Longer preamble	some	some	some
- ATDMA byte interleaving			X
- SCDMA spreading			X
- SCDMA de-spreading		X	
- SCDMA TCM	X		some
- Proprietary noise mitigation		X	

Table 3- DOCSIS Upstream Noise Mitigation Techniques & Corresponding Noise Types Mitigated

The impact of proprietary (Ingress) noise mitigation on the SNR and the PER for Ingress Noise was described above. The impact of the other noise mitigation techniques can be calculated as a modification to the Aggregate PER that was defined above.

The authors found that one could calculate the approximate changes to the Aggregate PER whenever one or more of these noise mitigation techniques are enabled. The inclusion of these changes leads to the Final PER that one would expect to see on the channel.

As an example of how the inclusion of another noise mitigation technique can be accommodated, let us consider the details behind the important noise mitigation technique known as Reed-Solomon Forward Error Correction (RS-FEC).

For TDMA and ATDMA and SCDMA US channels, the system operator has the option of enabling and configuring RS-FEC. RS-FEC is a very powerful noise mitigation technique that permits some symbol errors to be corrected at the receiver after they have been demodulated. The errors that are corrected could have initially been caused by AWGN, Ingress Noise, or Impulse Noise, so RS-FEC is very powerful (and very popular).

RS-FEC is a non-binary linear block code that encodes a block of k information bytes into a block of N transmitted bytes (N>k), where P=2T=(N-k) is the number of parity check bytes added into the transmitted block. (See **Fig. 6**).

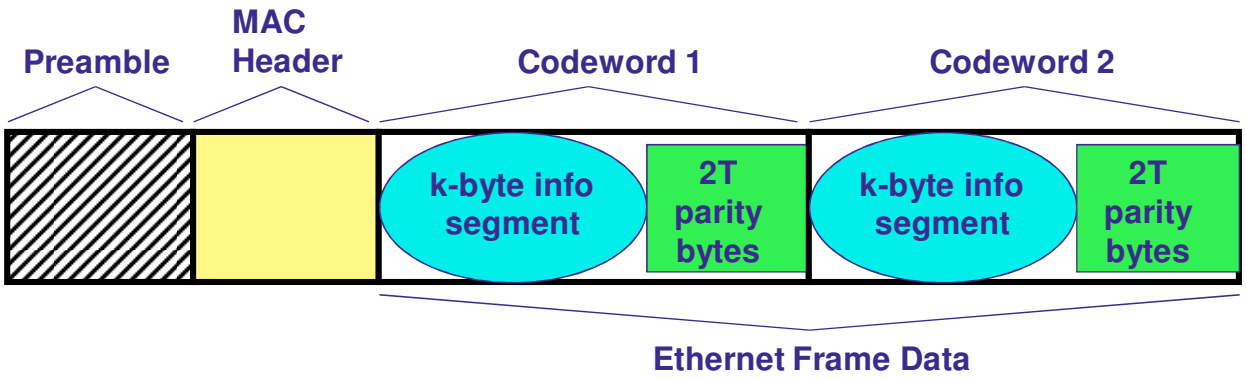

Fig. 6- DOCSIS MAC Frame Divided into Two RS-FEC Codewords, Each with k Bytes of Information and 2T Bytes of Parity

This RS-FEC block code is known as an (N,k) block code, and the N-byte entity that is transmitted is often called a codeword. With Reed-Solomon coding, the P parity check bytes can be used to correct errored bytes that arrive at the receiver. In particular, it can be shown that the presence of the P parity check bytes will permit $\left\lfloor T = \frac{P}{2} \right\rfloor$ errored bytes within a transmitted block to be corrected using Reed-Solomon coding. (Note: The floor function returns the largest integer value that is less than or equal to the function's argument).

For TDMA operation, the value of k (the number of information bytes within the codeword (i.e., the payload bytes excluding parity check bytes)) must be allowed to range from 16 bytes to 253 bytes, and the value of T (the number of correctable bytes within a single codeword) must be allowed to range from 0 bytes to 10 bytes, which will add P=2*T (ranging from P=0 to P=20) parity check bytes to the codeword.

For ATDMA and SCDMA operation, the value of k (the number of information bytes within the codeword (i.e., the payload bytes excluding parity check bytes)) must be allowed to range from 16 bytes to 253 bytes, and the value of T (the number of correctable bytes within a single codeword) must be allowed to range from 0 bytes to 16 bytes, which will add P=2*T (ranging from P=0 to P=32) parity check bytes to the codeword.

Once the byte error rate (Pbyte_errM… or Ptcm_byte_errM) for a particular channel has been calculated (taking Ingress Cancellation into account), it is relatively easy to create an expression for the Reed-Solomon codeword error rate (Pcodeword_errM). The equivalent codeword error rate Pcodeword_errM (after the implementation of the Reed-Solomon Forward Error Correction algorithm) can be determined from the byte error rate Pbyte_errM by recognizing the fact that a Reed-Solomon codeword containing N bytes (16 <= N <= 253) will be transmitted without error only if (N-T) or more bytes within the codeword were transmitted without error. Stated differently, a transmitted Reed-Solomon codeword with N bytes will experience an un-correctable error whenever more than T bytes arrive at the receiver in error.

The following derivation [Tri] can be used to determine an equation for Pcodeword_errM. We will consider a single "random experiment" to have one of two possible outcomes… success or failure. We will let the probability of success be p, and we will let the probability of failure be q. We will require that p+q=1. In our case, the "random experiment" will be the transmission of a single byte (within a Reed-Solomon codeword), and success is defined to be the un-errored transmission of the byte, while failure is defined to be the errored transmission of the byte.

Now consider a compound experiment consisting of a sequence of N independent repetitions of the original experiment. This sequence is known as a sequence of Bernoulli trials. In our case, the N independent trials represent the transmission of the N different bytes within a Reed-Solomon codeword.

If 1 denotes a successful outcome to an experiment and 0 denotes a failed outcome to an experiment, then the sample space for the N independent trials can be denoted by the set of 2^N different N-tuples of 0's and 1's. For example, if N=3, then there would be $2^3 = 8$ different 3-tuples that would make up the sample space:

{(0,0,0), (0,0,1), (0,1,0), (0,1,1), (1,0,0), (1,0,1), (1,1,0), (1,1,1)}

Any of the sample points (3-tuples) in the above set that has J 1's and (N-J) 0's had J successful experiments and (N-J) failed experiments, so it can be shown that the sample point will have a probability of occurrence given by $p^J \cdot q^{N-J}$. It should be noted that there are N!/[(J!)*(N-J)!] sample points with J 1's and (N-J) 0's, it can be shown that the probability of running the sequence of Bernoulli trials and experiencing exactly J successes is given by:

$$P(J) = \frac{N!}{J!(N-J)!} \cdot P^J \cdot q^{(N-J)} \qquad (11)$$

Recalling (from above) that a Reed-Solomon codeword containing N bytes (16 <= N <= 253) will be transmitted without error only if (N-T) or more bytes within the codeword were transmitted without error, we can use Eq. (11) to show that the probability that the N-byte Reed-Solomon codeword is transmitted without error is given by:

$$P_{codeword\_okM} = \sum_{i=N-T}^{N} P(i) \qquad (12)$$

$$P_{codeword\_okM} = \sum_{i=N-T}^{N} \frac{N!}{i!(N-i)!} \cdot P^i \cdot q^{(N-i)} \qquad (13)$$

But the values for p and q can be easily determined. p is the probability of a successful byte transmission, which is given by:

p = Pbyte_okM=(1- Pbyte_errM) (14)

q is the probability of an unsuccessful byte transmission, which is given by:

q = Pbyte_errM (15)

Substitution yields:

$$P_{codeword\_okM} = \sum_{i=N-T}^{N} \frac{N!}{i!-(N-i)!} \cdot \left(1 - P_{byte\_errM}\right)^{i} \cdot P_{byte\_errM}^{(N-i)} \quad (16)$$

We can also calculate:
Pcodeword_errM = 1-Pcodeword_okM (17)

Once the effect of Reed-Solomon Forward-Error Correction has been determined for the codewords, one may be interested in re-converting the probability of a codeword error into equivalent probabilities of error for differently-sized data chunks (ex: bit error rate or PER). Conversion formulae were described in an earlier section. Example results from the use of these RS-FEC calculations are illustrated in **Fig. 7**. It should be apparent from the figure that minor modifications in the T value for RS-FEC can have a very large impact on the Actual PER for a given SNR value.

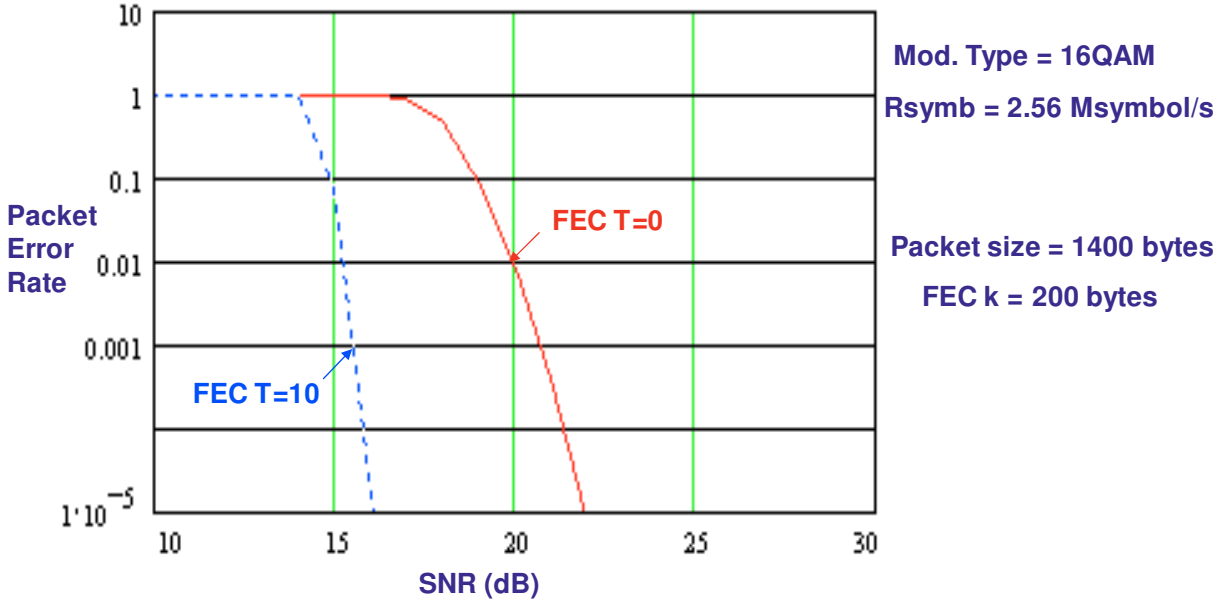

Fig. 7- Packet Error Rate as a function of SNR for different T values (in RS-FEC) with a 16QAM Channel

Similar formulae were developed and validated for all of the different noise mitigation techniques listed in **Table 3**.

Calculating the Actual Bandwidth Capacities in a DOCSIS Upstream Channel

In the previous sections, it was shown how various formulae could be used to predict the PER for a DOCSIS US Channel in the presence of any combination of noise types. The authors created a software-based analysis tool that could input the US Channel characteristics (which define the channel), the DOCSIS Modulation Profile characteristics (which define the signal on the channel), the signal power settings, and several finite-time samples of the noise that is present on the US Channel (as seen at the CMTS). The analysis tool parses through the noise samples and determines the magnitude and the nature of the different noise types on the channel. The tool then uses these noise parameters and the signal parameters to calculate a SNR for the channel. The tool then uses the aforementioned formulae to predict the Aggregate PER for the channel. The tool finally makes appropriate changes to the Aggregate PER prediction based on which noise mitigation techniques are enabled on the US Channel. This yields the Final PER prediction for the channel. The tool can then calculate the Actual Bandwidth Capacity that is available on the US Channel for subscriber use after the overhead of the various noise mitigation techniques is taken into account. As an example, an increase in the number of parity bytes (2T) used in a RS-FEC codeword can help to reduce the Final PER, but it also adds overhead to the channel. This overhead manifests itself as bytes transmitted across the US Channel that cannot be used to carry user data. As a result, the total number of user data bytes that are transmitted across the US Channel within a given window of time is effectively reduced, yielding a lower Actual Bandwidth Capacity available on the US Channel for subscriber use.

All of the above calculations can be done very rapidly by the software-based analysis tool, and the resulting Final PER and the resulting Actual Bandwidth Capacity are useful numbers that can be used to determine the quality of the channel. In an ideal world, the system operator would typically like the Final PER to be very low (to permit good TCP performance) and the Actual Bandwidth Capacity to be high (to permit fast downloads and uploads). However, a low SNR on the US Channel will typically make this desirable arrangement impossible to achieve, because the noise mitigation techniques used to overcome the high Aggregate PER (that results from the low SNR) will typically reduce the Actual Bandwidth Capacity (due to the overhead from the noise mitigation techniques).

Identifying the Optimal Settings in a DOCSIS Upstream Channel

A question that often comes to mind among system operators is whether a particular set of channel settings and a particular set of noise mitigation techniques are optimal for a particular US Channel with a particular type of noise. In other words, are there different channel settings and different noise mitigation techniques that could be employed on the US Channel with the noise which would yield a lower Final PER and a higher Actual Bandwidth Capacity? This question is a complex question, because there are many different combinations of channel settings and noise mitigation techniques that can be employed on a particular US Channel and a particular noise source. In essence, the number of "knobs" that the system operator must tune to achieve optimal performance on the US Channel is quite large (and quite intimidating). In particular, two different categories of "knobs" must be managed:

Modulation Profile Parameters (Burst Attributes defined for each Interval Usage Code or IUC):

- Modulation Type (QPSK, 8QAM, 16QAM, 32QAM, 64QAM, 128QAM)
- Differential Encoding On/Off
- Preamble Length
- Preamble Offset
- Reed-Solomon FEC Correctable Bytes (T)
- Reed-Solomon FEC Information Bytes per Codeword (k)
- Scrambler SEED
- Maximum Burst Size
- Guard Time Size
- Shortened Last Codeword On/Off
- Scrambler On/Off
- ATDMA Reed-Solomon Interleaver Depth
- ATDMA Reed-Solomon Interleaver Block Size
- Preamble Type
- SCDMA Spreader On/Off
- SCDMA Framer Codes Per Subframe
- SCDMA Framer Interleaver Step Size
- TCM Encoding On/Off (Off)

Channel TLV Parameters:

- Modulation Rate (160 Ksymbol/sec, 320 Ksymbol/sec, 640 Ksymbol/sec, 1.28 Msymbol/sec, 2.56 Msymbol/sec, 5.12 Msymbol/sec)
- Center Frequency
- Preamble Pattern
- Extended Preamble Pattern
- SCDMA Mode Enable
- SCDMA Spreading Intervals per Frame
- SCDMA Codes per Minislot
- SCDMA Number of Active Codes
- SCDMA Code Hopping Seed
- SCDMA Upstream Ratio Numerator
- SCDMA Upstream Ratio Denominator
- SCDMA Timestamp Snapshot
- Maintain Power Spectral Density
- Ranging Required

The authors decided that finding the optimal settings for all of these knobs (in the presence of a particular type of noise) was a time-consuming task that could only be done in an automated fashion. As a result, the analysis tool described above was augmented to search through the large multi-dimensional design space of channel parameters and noise mitigation tools to identify combinations of settings that would yield optimal performance levels, i.e., acceptable Final PER

levels and the highest permissible Actual Bandwidth Capacities. A high-level flowchart for the tasks performed by the analysis tool is shown in **Fig. 8**.

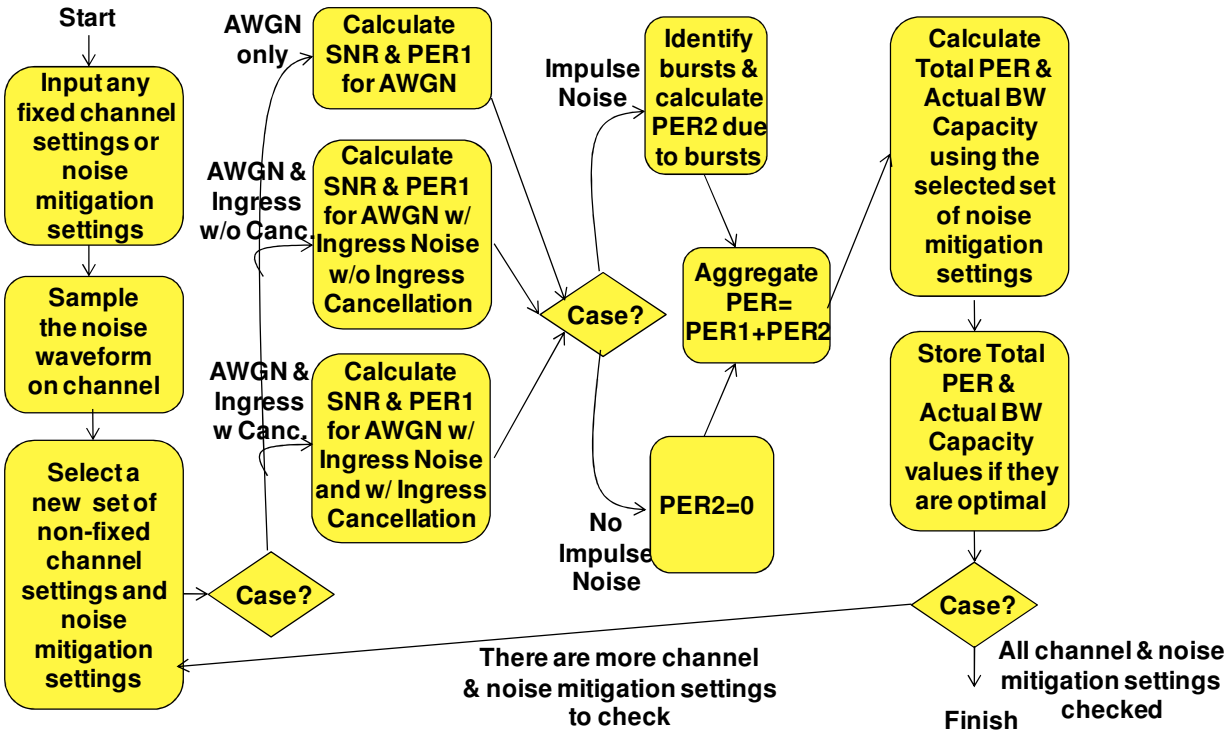

Fig. 8- Flowchart for Analysis Tool

Experience in using the analysis tool has shown that many of the improvements (due to setting optimizations) occur as a result of carefully-crafted trade-offs made between the ATDMA/SCDMA settings, the Modulation Type settings, the k value settings for RS-FEC, the T value settings for RS-FEC, and the Modulation Rate settings.

Comparing the Performance Levels of Bonded and Non-Bonded DOCSIS Upstream Channels

With the availability of the analysis tool described in the sections above, the authors have created the ability to rapidly calculate the maximum Actual Bandwidth Capacity of any DOCSIS US Channel in the presence of different noise types. The analysis tool also identifies the optimal channel settings and noise mitigation settings for the channel and the noise. All of these calculations can be constrained by a minimum PER level that must be maintained on the channel.

In this section, the authors will use the aforementioned analysis tool to compare the performance of Bonded and Non-Bonded DOCSIS US Channels in the presence of various noise types (AWGN, Semi-Additive White Gaussian Noise, Ingress Noise, and Impulse Noise). In particular, the authors will explore an interesting question that is created by the availability of Channel Bonding for the DOCSIS US. That question is: If a pass-band of (say) 6.4 MHz is available for

DOCSIS US transmission, is it better to set up a single 6.4 MHz channel or is it better to set up four bonded 1.6 MHz channels? (See **Fig. 9**). (Note: In the comparison, the authors have kept the CMTS Received Power Level settings for each of the US Channels within the analysis at the same level of 0 dBmV. This matches the approach that would likely be used by system operators. One of the reasons why a system operator might reduce the power level on the narrow channels would be to circumvent clipping issues at return lasers). As a result of maintaining the power levels in all of the channels, the power in any one of the four narrow channels will be equal to the power in the single wide channel, and the aggregated power in the four narrow channels will be four times higher than the power in the single wide channel.

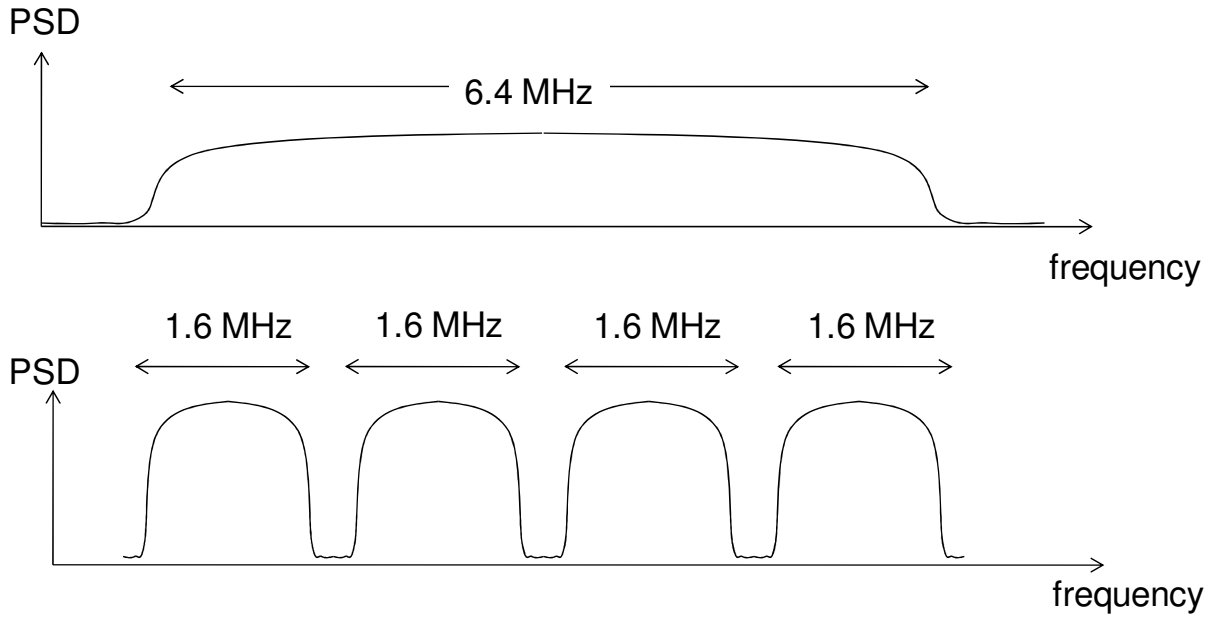

Fig. 9- Single Wide Channel vs. Four Narrow Channels (Channel Bonded)

The above question can be answered in several ways. From a cost point-of-view, it should be apparent that the use of four burst receivers at the CMTS will likely cost more than the use of one burst receiver. From a performance point-of-view, though, the answer is not as straight-forward.

Noise-Free Upstream Channels

In the absence of noise, the performance (Actual Bandwidth Capacity) of one 6.4 MHz US Channel running 16QAM is identical to the performance (Actual Bandwidth Capacity) of four bonded 1.6 MHz Channels running 16QAM. The single 6.4 MHz/16QAM US Channel supports a bandwidth of 20.48 Mbps. A single 1.6 MHz/16QAM US Channel supports a bandwidth of 5.12 Mbps, so four of these channels would support a bandwidth of 20.48 Mbps (which is identical to the bandwidth on the single 6.4 MHz/16QAM US Channel).

Upstream Channels in the Presence of AWGN

The authors were interested in analyzing and comparing the performance (Actual Bandwidth Capacity) of one 6.4 MHz US Channel to the performance (Actual Bandwidth Capacity) of four bonded 1.6 MHz Channels when the noise on the channel was AWGN noise like the noise shown in **Fig. 10**. For each of the channels, the analysis tool was configured to keep the Total PER level held to a value less than 1%.

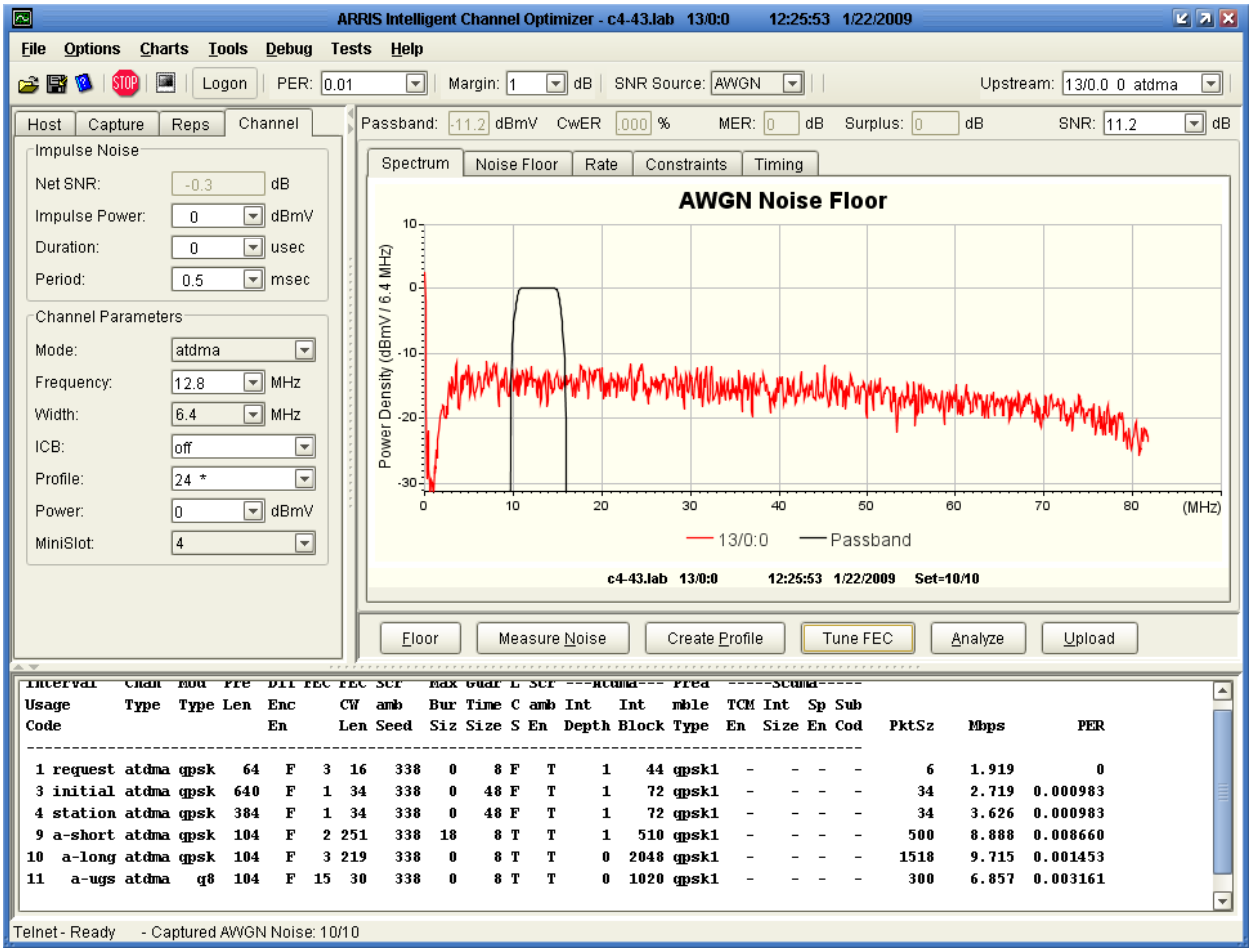

Fig. 10- Power Spectral Density of AWGN Sample

Since the received signal power level in any single channel is assumed to be held at a constant level of 0 dBmV, and since the amount of noise power passing through to the CMTS receiver is proportional to the width of the channel's pass-band, the noise on the wider 6.4 MHz channel is roughly four times higher than on each narrow 1.6 MHz channel. As a result, the SNR of the wider 6.4 MHz channel is always ~4 times lower than the SNR of each narrow 1.6 MHz channel. This permits the analysis tool to attempt the use of higher-order modulation types and less RS-FEC parity bytes to achieve the desired 1% PER on each narrow 1.6 MHz channel, while the tool must usually use lower-order modulation types and more RS-FEC parity bytes on the wider 6.4 MHz channel. For the noise floor shown in **Fig. 10** above, the analysis tool found that the wider

6.4 MHz channel could be tuned to QPSK modulation types and moderate RS-FEC parity to produce the optimal Actual Bandwidth Capacity. It also found that the four narrow 1.6 MHz channels could be tuned to 16QAM modulation types and stronger RS-FEC parity to produce the optimal Actual Bandwidth Capacities. The optimal Actual Bandwidth Capacities for each of these channels (as calculated by the analysis tool) are shown in **Table 4** below.

Channel	Modulation Type	RS-FEC	Optimal Actual Bandwidth Capacity (Mbps)
6.4 MHz channel	QPSK	Moderate (small T)	9.72
1.6 MHz channel #1	16QAM	Strong (large T)	4.73
1.6 MHz channel #2	16QAM	Strong (large T)	4.69
1.6 MHz channel #3	16QAM	Strong (large T)	4.60
1.6 MHz channel #4	16QAM	Strong (large T)	4.60
Σ(Four 1.6 MHz channels)			18.62

Table 4- Channels and Optimal Bandwidths with AWGN

It is interesting to note that the total Actual Bandwidth Capacity on the four 1.6 MHz bonded channels is approximately twice the bandwidth provided by the single 6.4 MHz channel. Since both examples use the same 6.4 MHz of bandwidth, it is clear that the use of Channel Bonding within a fixed pass-band can yield substantial bandwidth improvements in the presence of AWGN.

Upstream Channels in the Presence of Semi-AWGN

The authors were interested in analyzing and comparing the performance (Actual Bandwidth Capacity) of one 6.4 MHz US Channel to the performance (Actual Bandwidth Capacity) of four bonded 1.6 MHz Channels when the noise on the channel was Semi-AWGN. There are many different flavors of Semi-AWGN that one could imagine, so the authors opted to use the noise shown in **Fig. 11**. For each of the channels, the analysis tool was configured to keep the Total PER level held to a value less than 1%.

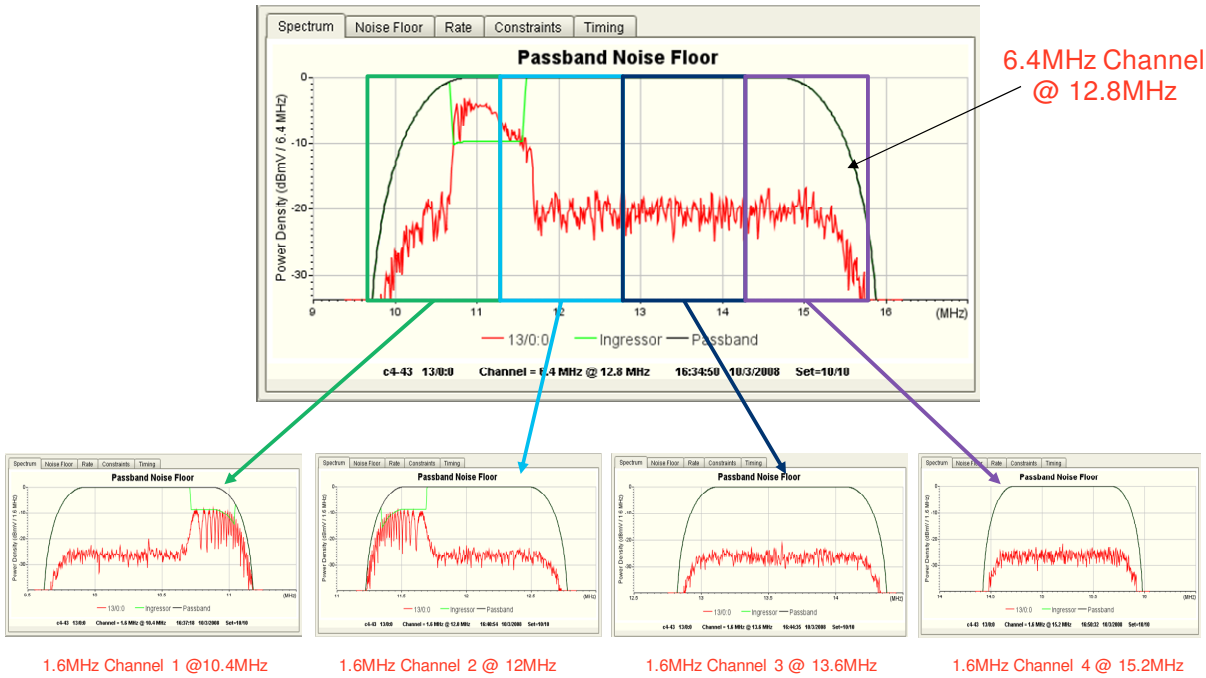

Fig. 11- Power Spectral Density of Semi-AWGN Sample

The analysis tool was allowed to determine the optimal Actual Bandwidth Capacities for each of these channels in the presence of the above noise type with Ingress Cancellation enabled. The results are shown in Table 5 below.

Channel	Optimal Actual Bandwidth Capacity (Mbps)
6.4 MHz channel	19.24
1.6 MHz channel #1	5.78
1.6 MHz channel #2	5.78
1.6 MHz channel #3	7.30
1.6 MHz channel #4	7.30
Σ(Four 1.6 MHz channels)	26.16

Table 5- Channels and Optimal Bandwidths with Semi-AWGN & Ingress Cancellation Enabled

The analysis tool was also allowed to determine the optimal Actual Bandwidth Capacities for each of these channels in the presence of the above noise type with Ingress Cancellation disabled. The results are shown in Table 6 below.

Channel	Optimal Actual Bandwidth Capacity (Mbps)
6.4 MHz channel	13.88
1.6 MHz channel #1	4.83
1.6 MHz channel #2	5.31
1.6 MHz channel #3	7.30
1.6 MHz channel #4	7.30
Σ(Four 1.6 MHz channels)	24.74

Table 6- Channels and Optimal Bandwidths with Semi-AWGN & Ingress Cancellation Disabled

It is interesting to note that the total Actual Bandwidth Capacity on the four 1.6 MHz bonded channels is always higher than the bandwidth provided by the single 6.4 MHz channel. Since both examples use the same 6.4 MHz of bandwidth, it is clear that the use of Channel Bonding within a fixed pass-band can yield substantial bandwidth improvements in the presence of Semi-AWGN.

Upstream Channels in the Presence of Ingress Noise

The authors were interested in analyzing and comparing the performance (Actual Bandwidth Capacity) of one 6.4 MHz US Channel to the performance (Actual Bandwidth Capacity) of four bonded 1.6 MHz Channels when the channel contained Ingress Noise. There are many different flavors of Ingress Noise that one could imagine, so the authors opted to use the noise shown in **Fig. 12**. For each of the channels, the analysis tool was configured to keep the Total PER level held to a value less than 1%.

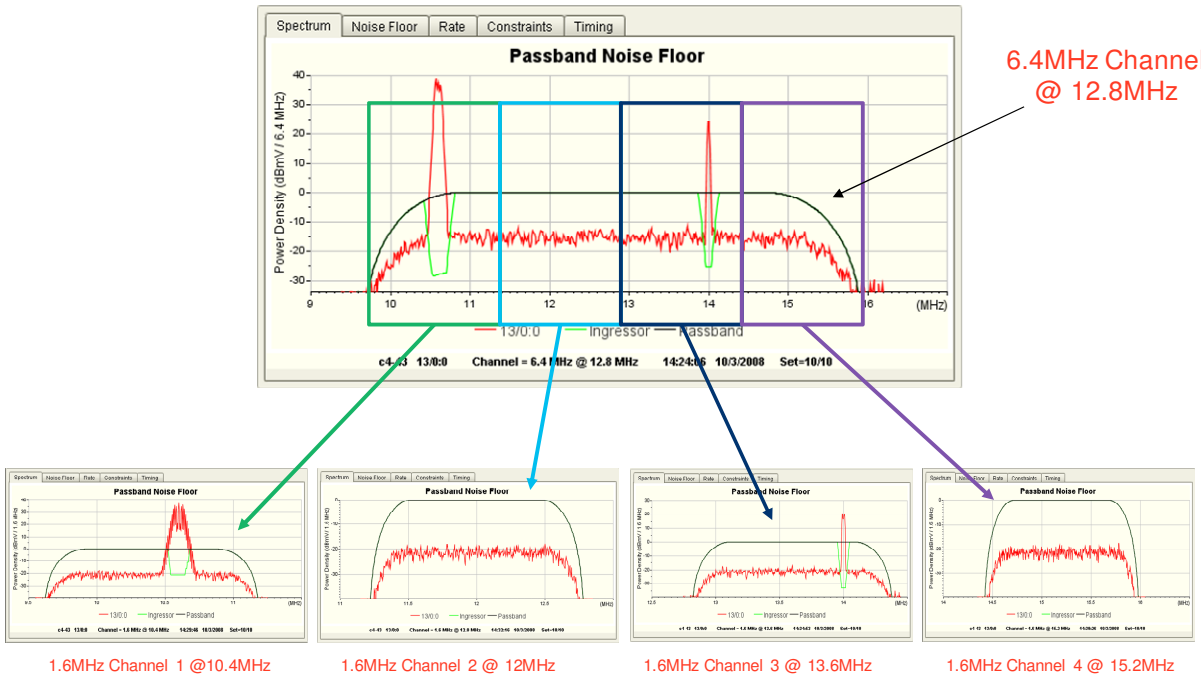

Fig. 12- Power Spectral Density of Ingress Noise Sample

The analysis tool was allowed to determine the optimal Actual Bandwidth Capacities for each of these channels in the presence of the above noise type with Ingress Cancellation enabled. The results are shown in Table 7 below.

Channel	Optimal Actual Bandwidth Capacity (Mbps)
6.4 MHz channel	6.39
1.6 MHz channel #1	0.00
1.6 MHz channel #2	6.79
1.6 MHz channel #3	6.48
1.6 MHz channel #4	6.79
Σ(Four 1.6 MHz channels)	20.06

Table 7- Channels and Optimal Bandwidths with Ingress Noise & Ingress Cancellation Enabled

The analysis tool was also allowed to determine the optimal Actual Bandwidth Capacities for each of these channels in the presence of the above noise type with Ingress Cancellation disabled. The results are shown in Table 8 below.

Channel	Optimal Actual Bandwidth Capacity (Mbps)
6.4 MHz channel	0.00
1.6 MHz channel #1	0.00
1.6 MHz channel #2	6.79
1.6 MHz channel #3	0.00
1.6 MHz channel #4	6.79
Σ(Four 1.6 MHz channels)	13.58

Table 8- Channels and Optimal Bandwidths with Semi-AWGN & Ingress Cancellation Disabled

It is interesting to note that the total Actual Bandwidth Capacity on the four 1.6 MHz bonded channels is always higher than the bandwidth provided by the single 6.4 MHz channel. Since both examples use the same 6.4 MHz of bandwidth, it is clear that the use of Channel Bonding within a fixed pass-band can yield substantial bandwidth improvements in the presence of Ingress Noise.

Upstream Channels in the Presence of Impulse Noise

The authors were interested in analyzing and comparing the performance (Actual Bandwidth Capacity) of one 6.4 MHz US Channel to the performance (Actual Bandwidth Capacity) of four bonded 1.6 MHz Channels when the channel contained Impulse Noise. There are many different flavors of Impulse Noise that one could imagine, so the authors opted to use the noise shown in **Fig. 13**. For each of the channels, the analysis tool was configured to keep the Total PER level held to a value less than 1%.

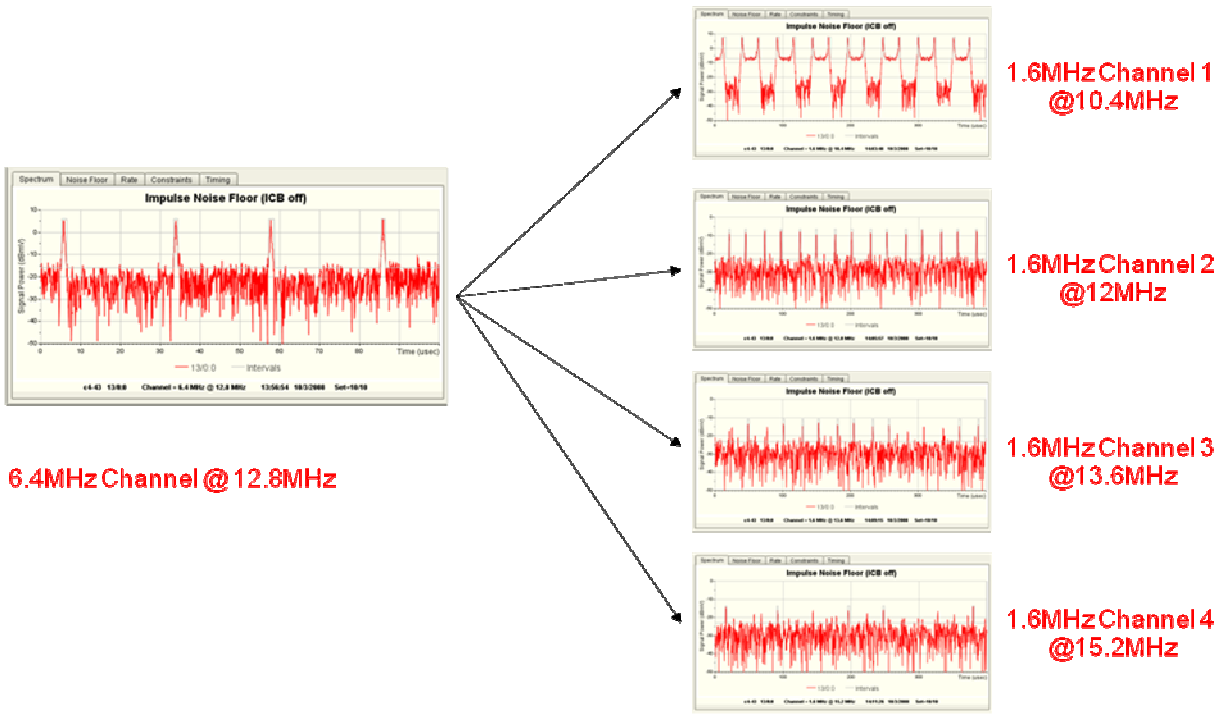

Fig. 13- Power Spectral Density of Impulse Noise Sample

The analysis tool was allowed to determine the optimal Actual Bandwidth Capacities for each of these channels in the presence of the above noise type. The results are shown in Table 9 below.

Channel	Optimal Actual Bandwidth Capacity (Mbps)
6.4 MHz channel	15.67
1.6 MHz channel #1	0.00
1.6 MHz channel #2	5.11
1.6 MHz channel #3	5.46
1.6 MHz channel #4	6.94
Σ(Four 1.6 MHz channels)	17.51

Table 9- Channels and Optimal Bandwidths with Impulse Noise

It is interesting to note that the total Actual Bandwidth Capacity on the four 1.6 MHz bonded channels is higher than the bandwidth provided by the single 6.4 MHz channel. Since both examples use the same 6.4 MHz of bandwidth, it is clear that the use of Channel Bonding within a fixed pass-band can yield some bandwidth improvements in the presence of Impulse Noise.

Impact on Future DOCSIS Deployments

If MSOs opted to use the narrow-channel Channel Bonding concepts described in this paper to optimize the throughput performance of their US Channels, it would obviously imply a need for more US transmitters in the CMs and more US burst receivers in the CMTS.

For example, let us consider a hypothetical scenario in which an MSO had been planning to deploy US Channel Bonding to a particular Service Group using four wide 6.4 MHz US Channels. Using the proposal within this paper, the MSO would instead deploy US Channel Bonding using many narrow 1.6 MHz US Channels. As a result, CMs operating in this Service Group would have to support more than four US transmitters and the CMTS connected to this Service Group would have to support more than four burst receivers for the Service Group.

An obvious question results from the above hypothetical scenario. In particular, how much more capacity (US transmitters and US burst receivers) would need to be supported in the CMs and the CMTSs of the future to support the use of the narrow US Channels in a Channel Bonding environment. This question is somewhat difficult to answer, because the answer depends on a lot of variable factors, such as the expected size of the headend, the expected DS:US bandwidth ratios in the CMTS, and the actual bandwidths consumed by the subscribers in the headend. However, we can make some assumptions to give us some rough guidelines.

Using projections from [Clo], we will assume that a typical DOCSIS subscriber in ~7 years will consume an average DS bandwidth of ~3.5 Mbps. Using recent DS:US bandwidth ratio measurements from several MSOs and assuming those ratios will remain constant moving forward into the future, we will assume that a typical DS:US bandwidth ratio of the future will be ~4:1. As a result, we might predict that the average US bandwidth per DOCSIS subscriber may be ~875 kbps in ~7 years. Assume a "typical" headend of the future will support (say) 20K households-passed arranged across 80 Service Groups with 250 households each. If the DOCSIS take-rate in the future is 30%, then each of the 80 Service Groups will have an average of (250)*(30%) = 75 DOCSIS subscribers. If each DOCSIS subscriber consumes an average of 3.5 Mbps of DS bandwidth and 875 kbps of US bandwidth, then each of the 80 Service Groups must be supplied with (75)*(3.5 Mbps) = 262 Mbps of DS bandwidth capacity and (75)*(875 kbps) = 65 Mbps of US bandwidth capacity. The DS bandwidth capacity to each Service Group could therefore be provided by (262 Mbps/~40 Mbps) = seven 256QAM Annex B DOCSIS DS Channels. If we assume that the noise in the US spectrum is similar to the noise shown in **Fig. 10** (with resulting bandwidth capacities similar to the values shown in **Table 4**), then the required US bandwidth for the Service Group could be provided by (65 Mbps/~9.72 Mbps) = seven 6.4 MHz US 6.4 MHz Channels (consuming 44.8 MHz of US spectrum). Or using the narrow-channel Channel Bonding proposal of this paper, the required US bandwidth for the Service Group could be provided by (65 Mbps/18.62 Mbps)*4 = fourteen 1.6 MHz US Channels (consuming 22.4 MHz of US spectrum). Interestingly, the approach based on seven wide 6.4 MHz channels would not fit in the 5-42 MHz US pass-band, so it would require some form of

US augmentation (such as a mid-split architecture). However, the approach based on the narrow-channel Channel Bonding proposal with fourteen 1.6 MHz channels would easily fit in the 5-42 MHz US pass-band, and would therefore not require any US augmentation like mid-splits. This fact alone could be reason enough for MSOs to consider the use of the proposed narrow-channel Channel Bonding approach.

In the narrow-channel Channel Bonding scenario above, CMs used in each Service Group would obviously need to support at least seven DS receivers and fourteen US transmitters. The CMTS connected to each Service Group would also need to dedicate seven DS transmitters and fourteen US burst receivers to the Service Group. Thus, a single CMTS supporting the 80 Service Groups would need to provide (80)*(7) = 560 DS transmitters and (80)*(14) = 1120 US burst receivers.

Challenges

Even though there are clear benefits associated with the use of the narrow-channel Channel Bonding proposal, there are also several challenges that can be found within the narrow-channel Channel Bonding scenario described in the previous section.

First, MSOs must be able to deploy the large number of DS Channels and US Channels within their available spectrum. Freeing up seven DS Channels within their DS spectrum for DOCSIS applications should be possible with the ongoing reclamation of analog channels. In addition, the US spectrum for the fourteen 1.6 MHz US Channels should be available on the 5-42 MHz pass-band within their already-deployed HFC plants.

Second, there must be adequate DS bandwidth capacity to support all of the "overhead bandwidth" generated by the MAC Management messaging. This "overhead bandwidth" includes MAPs, SYNCs, MDDs, UCDs, and Ranging Messages. Tests and measurements on working DOCSIS systems have shown that MAPs dominate the "overhead bandwidth." While the "overhead bandwidth" can vary depending on CMTS configuration settings, "typical" measurements indicate that the CMTS may inject ~200 kbps of MAPs on the primary DS Channel for each US Channel that is being managed. As a result, the narrow-channel Channel Bonding scenario described in the previous section would inject (14)*(~200 kbps) = ~2.8 Mbps. This small amount of "overhead bandwidth" within a 7-channel DS Bonding Group (providing ~280 Mbps of total DS bandwidth capacity) does not seem excessive, so there should be adequate bandwidth capacity to support the "overhead bandwidth."

Third, MSOs must be able to provide the large number of CMTS US burst receivers (and CMTS DS transmitters) at a reasonable cost. This is a challenge that is already being worked on by next-generation CMTS vendors. While the large CMTS capacity numbers may seem high by today's CMTS standards, CMTS vendors should be able to achieve these capacities by capitalizing on the benefits of Moore's Law over the next few years.

Fourth, MSOs must be able to deploy CMs with at least seven DS receivers and fourteen US transmitters at a reasonable cost. This is a challenge that is already being worked on by next-generation CM vendors, and it is already apparent that these numbers should be achievable within the next several years.

Finally, the return lasers used by the MSOs must be able to support the aggregated power level resulting from the frequency-division multiplexing of the fourteen US channels without excessive distortion or clipping. This is an issue that will need to be addressed in the future. If existing lasers are not able to provide this functionality, then more exotic techniques (like moving the DOCSIS US PHY into the Fiber Node) might be required.

Conclusions

This paper compared the performance of both wide non-bonded US Channels and multiple, narrow channel-bonded US Channels. In particular, the authors studied the performance (Actual Bandwidth Capacities) for a single 6.4 MHz channel and for four 1.6 MHz bonded channels positioned at the same location in the frequency spectrum as the single 6.4 MHz channel. Various types of noise waveforms (AWGN, Semi-AWGN, Ingress Noise, and Impulse Noise) were introduced into the spectrum of the channels, and the optimal Actual Bandwidth Capacities of each of the channels was calculated assuming:

1) The Received Power Level at the CMTS was maintained at 0 dBmV for each channel, and

2) The Packer Error Rate on each channel was kept at a level below 1%.

For all of the different noise types used in the study, it was found that the total Actual Bandwidth Capacity provided by the four bonded 1.6 MHz channels was greater than the Actual Bandwidth Capacity provided by the single non-bonded 6.4 MHz channel. It should be noted that this capacity gain is *in addition to* the well-known statistical multiplexing gains that are also introduced by the creation of larger channels.

The capacity gains were modest for the employed Impulse Noise waveforms. However, they were quite large for the employed AWGN, Semi-AWGN, and Ingress Noise waveforms. In fact, for the Semi-AWGN waveform used with the Ingress Cancellation features disabled, the Actual Bandwidth Capacity for the single 6.4 MHz channel was zero (due to the excessive distortion resulting from the Semi-AWGN). The same situation for the four bonded 1.6 MHz channels yielded a total Actual Bandwidth Capacity of 13.58 Mbps, because three of the four narrow channels were able to pass traffic by circumventing the noisy portion of the spectrum.

This paper only analyzed a small subset of noise waveforms. Many other noise waveforms could exist on a real HFC plant. Nevertheless, from the results presented in this paper, one can conclude that the use of multiple narrow channel-bonded channels may oftentimes yield much

higher bandwidth capacities than the use of a single wide non-bonded channel for many different noise waveforms that can exist on the HFC plant.

Acknowledgements

The authors would like to thank Carol Ansley, Tony Cotter, Ruth Cloonan, Alan Doucette, Greg Gohman, Bill Hanks, and Jeff Howe for input and guidance on some of the real-world bandwidth parameters.

References

[Clo] T. J. Cloonan, "On the Evolution of the HFC Network and the DOCSIS CMTS: A Roadmap for the 2012-2016 Era," Proceedings, SCTE 2008 Cable Tec-Expo (June, 2008).

[Pro] J. G. Proakis, Digital Communications, McGraw-Hill, 2001.

[Sch] M. Schwartz, Information Transmission, Modulation, and Noise, McGraw-Hill, 1980.

[Skl] B. Sklar, Digital Communications, Fundamentals and Applications, Prentice Hall, 2001.

[Sta] H. Stark and J. Woods, "Probability and Random Processes with Application to Signal Processing," Third edition, Prentice-Hall, 2002.

[Str] F. G. Stremler, Introduction to Communication Systems, Addison-Wesley, 1977.

[Tri] K. S. Trivedi, Probability and Statistics with Reliability, Queuing, and Computer Science Applications. Prentice-Hall, 1982.

List of Abbreviations and Acronyms

ATDMA	Advanced Time Division Multiple Access
AWGN	Additive White Gaussian Noise
BW	Bandwidth
CM	Cable Modem
CMTS	Cable Modem Termination System
DOCSIS	Data Over Cable Service Interface Specification
Eavg	Energy per symbol
Eb	Energy per bit
dB	decibel
DS	Downstream
MAC	Media Access Control Layer
Mbps	Megabits per second
MDD	MAC Domain Descriptor Message
MHz	MegaHertz

MSO	Multiple System Operator
Pavg	Average Power
PER	Packet Error Rate
PHY	Physical Layer
PSD	Power Spectral Density
QAM	Quadrature Amplitude Modulation
QPSK	Quadrature Phase Shift Keying
QoS	Quality of Service
RS-FEC	Reed-Solomon Forward Error Correction
Rsymb	Symbol Rate
SCDMA	Synchronous Code Division Multiple Access
SNR	Signal to Noise Ratio
SYNC	Synchronization Message
Ta	Symbol Period
TCM	Trellis Coded Modulation
TDMA	Time Division Multiple Access
UCD	Upstream Channel Descriptor Message
US	Upstream